AAS 09-153

DISPLACED PERIODIC ORBITS WITH LOW-THRUST PROPULSION IN THE EARTH-MOON SYSTEM

Jules Simo* **and Colin R. McInnes†**

Solar sailing and solar electric technology provide alternative forms of spacecraft propulsion. These propulsion systems can enable exciting new space-science mission concepts such as solar system exploration and deep space observation. The aim of this work is to investigate new families of highly non-Keplerian orbits, within the frame of the Earth-Moon circular restricted three-body problem (CRTBP), where the third massless body utilizes a hybrid of solar sail and a solar electric thruster. The augmented thrust acceleration is applied to ensure a constant displacement periodic orbit above L_2, leading to simpler tracking from the lunar surface for communication applications. Using an approximate, first order analytical solution to the nonlinear non-autonomous ordinary differential equations, periodic orbits can be derived that are displaced above/below the plane of the CRTBP.

INTRODUCTION

The use of solar electric propulsion (SEP) technology is now a realistic option for designing trajectories for interplanetary missions, while solar sail technology is currently under development. The topics covered in this paper are the results of displaced periodic orbits in the Earth-Moon system in which the third body uses a hybrid solar sail. The hybrid sail model is composed of two low thrust propulsion systems, namely a solar sail and solar electric propulsion.

A solar sail is propelled by reflecting solar photons; transforming the momentum of the photons into a propulsive force. Solar sail technology appears as a promising form of advanced spacecraft propulsion which can enable exciting new space-science mission concepts such as solar system exploration and deep space observation. This form of propulsion can provide energy changes greater than are possible with either ion or chemical propellants. Solar sails can also be utilised to maintain highly non-Keplerian orbits, such as closed orbits displaced high above the ecliptic plane (see McInnes,[1] Waters and McInnes,[2] Simo and McInnes[3]). Solar sails are especially suited for such non-Keplerian orbits, since they can apply a propulsive force continuously over indefinitely long periods. In such trajectories, a sail can be used as a communication satellite for high latitudes. For example, the orbital plane of the sail can be displaced above the orbital plane of the Earth, so that the sail can stay fixed above the Earth at some distance, if the orbital periods are equal. McInnes[4] investigated a new family of displaced solar sail orbits near the Earth-Moon libration points. Displaced orbits have more recently been developed by Ozimek et al.[5] using collocation methods. In Baoyin and McInnes[6,7,8] and McInnes[4,9], the authors describe new orbits which are associated with artificial lagrange points in the Earth-Sun system. These artificial equilibria have potential applications for future space physics and Earth observation missions. In McInnes and Simmons[10], the authors

*Research Fellow, Department of Mechanical Engineering, University of Strathclyde, Glasgow, G1 1XJ, United Kingdom. Email: jules.simo@strath.ac.uk.

†Professor, Department of Mechanical Engineering, University of Strathclyde, Glasgow, G1 1XJ, United Kingdom. Email: colin.mcinnes@strath.ac.uk.

investigate large new families of solar sail orbits, such as Sun-centered halo-type trajectories, with the sail executing a circular orbit of a chosen period above the ecliptic plane.

The idea of combining a solar sail with an auxiliary SEP system to obtain a hybrid sail system is important due to the challenges of performing complex missions (see Leipold and Götz,[11] Mengali and Quarta,[12] Baig and McInnes[13]). The solar electric propulsion system possess high specific impulse ($I_{sp} \approx 3000\ sec$). SEP consumes propellant and decreases the mass of the spacecraft, whereas the solar sail do not consume any propellant. Hence, one of the most important tasks during this analysis should be the control of the thrust as the propellant is consumed to obtain a constant acceleration. This form of propulsion is useful for some high energy missions, but unlike solar sails, they have a finite ΔV capability, which makes them unsuitable for missions where a non-Keplerian orbit has to be maintained over indefinite periods of time.

Orbits around the collinear libration points of the Earth-Moon system are of great interest because their unique positions are advantageous for several important applications in space mission design (see e.g. Szebehely[14], Farquhar,[15] Roy,[16] Vonbun,[17] Thurman et al.,[18] Gómez et al.,[19,20] Breakwell and Brown[21], Richardson[22], Howell[23,24]). Such orbits cannot be maintained without active control due to their instability (see Breakwell and Brown[21], Richardson[22], Howell[23,24]). If the orbit maintains visibility from Earth, a spacecraft on it (near the L_2 point) can be used to provide communications between the equatorial regions of the Earth and the lunar poles. Moreover, if another communications satellite is located at the L_1 point, there could be continuous communications coverage between the equatorial region of the Earth and the lunar surface (see Farquhar[25], Farquhar and Kamel[26]).

This paper investigates displaced periodic orbits at linear order in the circular restricted Earth-Moon system, where the third massless body utilizes a hybrid of solar sail and a solar electric propulsion. In particular, periodic motions in the vicinity of the Lagrange points in the Earth-Moon system will be explored along with their applications. Firstly we describe the dynamic model of the hybrid sail. The first-order approximation is derived for the linearized equations of motion. Then, a feedback linearization control scheme (see Slotine and Li[27]) is proposed and implemented. The main idea of this approach is to cancel the nonlinearities in a nonlinear system and to impose a desired linear dynamics. This provides the key advantage that the displacement distance of the hybrid sail is then constant. The displaced orbits found by Ozimek et al.[5] show large excursions in displacement distance. In practice, a constant displacement distance may lead to easier tracking from the lunar surface for communications applications. Unfortunately, the internal dynamics of the linear system are not always stable. Therefore, a stabilizing approach is used to increase the damping in the system and thereby to allow a higher gain in the controller. Finally, we evaluate the performance of the Hybrid Sail.

SYSTEM MODEL

In this work, we will assume that m_1 represents the larger primary (Earth), m_2 the smaller primary (Moon) and we will be concerned with the motion of a hybrid sail that has negligible mass. It is always assumed that the two more massive bodies (primaries) are moving in circular orbits about their common center of mass and the mass of the third body is too small to affect the motion of the two more massive bodies. The problem of the motion of the third body is the circular restricted three-body problem (CRTBP).

In order to develop any mathematical model without loss of the generality, it is useful to introduce

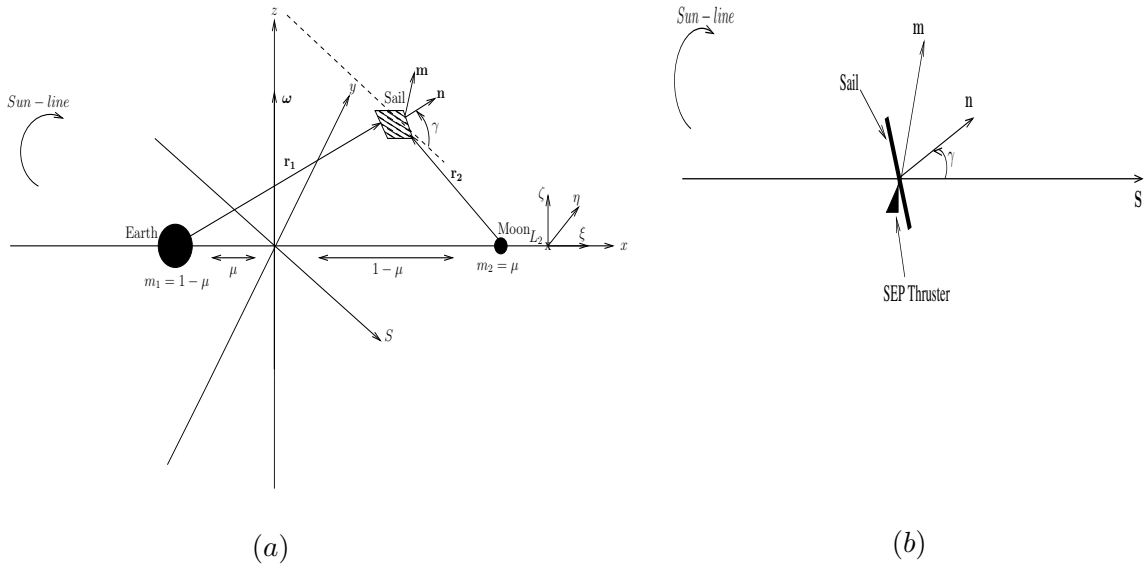

(a) (b)

Figure 1 (a) **Schematic geometry of the Hybrid Sail in the Earth-Moon restricted three-body problem;** (b) **Angle** γ **between the Hybrid Sail surface normal** ***n*** **and the Sun-line direction** ***S*****.**

some parameters that are characteristics of each particular three-body system. This set of parameters is used to normalize the equations of motion. The unit mass is taken to be the total mass of the system $(m_1 + m_2)$ and the unit of length is chosen to be the constant separation between m_1 and m_2. Under these considerations the masses of the primaries in the normalized system of units are $m_1 = 1 - \mu$ and $m_2 = \mu$, with $\mu = m_2/(m_1 + m_2)$ (see Figure 1 (a)).

Equations of Motions

The nondimensional equation of a motion of a hybrid sail in the rotating frame of reference is described by

$$\frac{d^2\boldsymbol{r}}{dt^2} + 2\boldsymbol{\omega} \times \frac{d\boldsymbol{r}}{dt} + \nabla U(\boldsymbol{r}) = \boldsymbol{a}_S + \boldsymbol{a}_{SEP}, \tag{1}$$

where $\boldsymbol{\omega} = \omega\hat{\boldsymbol{z}}$ ($\hat{\boldsymbol{z}}$ is a unit vector pointing in the direction $\boldsymbol{z}$) is the angular velocity vector of the rotating frame and $\boldsymbol{r}$ is the position vector of the hybrid sail relative to the center of mass of the two primaries. We will not consider the small annual changes in the inclination of the Sun line with respect to the plane of the system. The three-body gravitational potential $U(\boldsymbol{r})$, the solar radiation pressure acceleration $\boldsymbol{a}_S$ and the nondimensional acceleration due to the SEP thruster $\boldsymbol{a}_{SEP}$ are defined by

$$\begin{aligned} U(\boldsymbol{r}) &= -\left[\frac{1}{2}|\boldsymbol{\omega} \times \boldsymbol{r}|^2 + \frac{1-\mu}{r_1} + \frac{\mu}{r_2}\right], \\ \boldsymbol{a}_S &= a_0(\boldsymbol{S} \cdot \boldsymbol{n})^2\boldsymbol{n}, \qquad (2) \\ \boldsymbol{a}_{SEP} &= a_{SEP}\boldsymbol{m}, \qquad (3) \end{aligned}$$

where $\mu = 0.1215$ is the mass ratio for the Earth-Moon system. The hybrid sail position vectors w.r.t. m_1 and m_2 respectively (see Figure 1 (a)), are defined as $\boldsymbol{r}_1 = [x + \mu, y, z\ ]^T$ and $\boldsymbol{r}_2 = [x - (1-\mu), y, z]^T$, a_0 is the magnitude of the solar radition pressure acceleration exerted on the

hybrid sail and the unit vector $\boldsymbol{n}$ denotes the thrust direction, $\boldsymbol{a}_{SEP}$ is the acceleration from the SEP system and the unit vector $\boldsymbol{m}$ denotes the thrust direction. The sail is oriented such that it is always directed along the Sun-line $\boldsymbol{S}$, pitched at an angle γ to provide a constant out-of-plane force. The unit normal to the hybrid sail surface $\boldsymbol{n}$ and the Sun-line direction are given by

$$\begin{aligned} \boldsymbol{n} &= \left[\begin{array}{ccc} \cos(\gamma)\cos(\omega_\star t) & -\cos(\gamma)\sin(\omega_\star t) & \sin(\gamma) \end{array}\right]^T, \\ \boldsymbol{S} &= \left[\begin{array}{ccc} \cos(\omega_\star t) & -\sin(\omega_\star t) & 0 \end{array}\right]^T, \end{aligned}$$

where $\omega_\star = 0.923$ is the angular rate of the Sun-line in the corotating frame in a dimensionless synodic coordinate system.

Linearized System

We now want to investigate the dynamics of the hybrid sail in the neighborhood of the libration points. We denote the coordinates of the equilibrium point as $\boldsymbol{r}_L = (x_{L_i}, y_{L_i}, z_{L_i})$ with $i = 1, \cdots, 5$. Let a small displacement in $\boldsymbol{r}_L$ be $\delta\boldsymbol{r}$ such that $\boldsymbol{r} \rightarrow \boldsymbol{r}_L + \delta\boldsymbol{r}$. The equations for the hybrid sail can then be written as

$$\frac{d^2\delta\boldsymbol{r}}{dt^2} + 2\boldsymbol{\omega} \times \frac{d\delta\boldsymbol{r}}{dt} + \nabla U(\boldsymbol{r}_L + \delta\boldsymbol{r}) = \boldsymbol{a}_S(\boldsymbol{r}_L + \delta\boldsymbol{r}) + \boldsymbol{a}_{SEP}(\boldsymbol{r}_L + \delta\boldsymbol{r}), \tag{4}$$

and retaining only the first-order term in $\delta\boldsymbol{r} = [\delta x, \delta y, \delta y]^T$ in a Taylor-series expansion, the gradient of the potential and the acceleration can be expressed as

$$\nabla U(\boldsymbol{r}_L + \delta\boldsymbol{r}) = \nabla U(\boldsymbol{r}_L) + \left.\frac{\partial \nabla U(\boldsymbol{r})}{\partial \boldsymbol{r}}\right|_{\boldsymbol{r}=\boldsymbol{r}_L} \delta\boldsymbol{r} + O(\delta\boldsymbol{r}^2), \tag{5}$$

$$\boldsymbol{a}_S(\boldsymbol{r}_L + \delta\boldsymbol{r}) = \boldsymbol{a}_S(\boldsymbol{r}_L) + \left.\frac{\partial \boldsymbol{a}_S(\boldsymbol{r})}{\partial \boldsymbol{r}}\right|_{\boldsymbol{r}=\boldsymbol{r}_L} \delta\boldsymbol{r} + O(\delta\boldsymbol{r}^2). \tag{6}$$

$$\boldsymbol{a}_{SEP}(\boldsymbol{r}_L + \delta\boldsymbol{r}) = \boldsymbol{a}_{SEP}(\boldsymbol{r}_L) + \left.\frac{\partial \boldsymbol{a}_{SEP}(\boldsymbol{r})}{\partial \boldsymbol{r}}\right|_{\boldsymbol{r}=\boldsymbol{r}_L} \delta\boldsymbol{r} + O(\delta\boldsymbol{r}^2). \tag{7}$$

It is assumed that $\nabla U(\boldsymbol{r}_L) = 0$, and the accelerations $\boldsymbol{a}_S$ and $\boldsymbol{a}_{SEP}$ are constant with respect to the small displacement $\delta\boldsymbol{r}$, so that

$$\left.\frac{\partial \boldsymbol{a}_S(\boldsymbol{r})}{\partial \boldsymbol{r}}\right|_{\boldsymbol{r}=\boldsymbol{r}_L} = 0, \tag{8}$$

$$\left.\frac{\partial \boldsymbol{a}_{SEP}(\boldsymbol{r})}{\partial \boldsymbol{r}}\right|_{\boldsymbol{r}=\boldsymbol{r}_L} = 0. \tag{9}$$

The linear variational system associated with the libration points at $\boldsymbol{r}_L$ can be determined through a Taylor series expansion by substituting Eqs. (5) and (6) into (4) so that

$$\frac{d^2\delta\boldsymbol{r}}{dt^2} + 2\boldsymbol{\omega} \times \frac{d\delta\boldsymbol{r}}{dt} + K\delta\boldsymbol{r} = 0, \tag{10}$$

where the time-dependant matrix K is defined as

$$K = \left[\left.\frac{\partial \nabla U(\boldsymbol{r})}{\partial \boldsymbol{r}}\right|_{\boldsymbol{r}=\boldsymbol{r}_L} - \boldsymbol{a}_S(\boldsymbol{r}_L) - \boldsymbol{a}_{SEP}(\boldsymbol{r}_L)\right]. \tag{11}$$

Using matrix notation the linearized equation about the libration point (Equation (10)) can be represented by the homogeneous linear system $\dot{\mathbf{X}} = A(t)\mathbf{X}$, where the state vector $\mathbf{X} = (\delta\boldsymbol{r}, \delta\dot{\boldsymbol{r}})^T$, and for which the coefficients of the matrix $A(t) = A(t+T)$ are periodic functions of time with period $T = 2\pi/\omega_\star$.

The Jacobian matrix $A(t)$ has the general form

$$A(t) = \begin{pmatrix} 0_3 & I_3 \\ K & \Omega \end{pmatrix}, \tag{12}$$

where I_3 is a identity matrix, and

$$\Omega = \begin{pmatrix} 0 & 2 & 0 \\ -2 & 0 & 0 \\ 0 & 0 & 0 \end{pmatrix}. \tag{13}$$

Again, the sail attitude is fixed such that the sail normal vector $\boldsymbol{n}$, which is the unit vector that is perpendicular to the sail surface, points always along the direction of the Sun line with the following constraint $\boldsymbol{S} \cdot \boldsymbol{n} \geq 0$. Its direction is described by the pitch angle γ relative to the Sun-line, which represents the sail attitude. By making the transformation $\boldsymbol{r} \rightarrow \boldsymbol{r}_L + \delta\boldsymbol{r}$ and retaining only the first-order term in $\delta\boldsymbol{r} = (\xi, \eta, \zeta)^T$ in a Taylor-series expansion where (ξ, η, ζ) are axes attached to the libration point as shown in Figure 1 (a), the linearized nondimensional equations of motion relative to the collinear libration points can be written as

$$\ddot{\xi} - 2\dot{\eta} - U^o_{xx}\xi = a_\xi + a_{SEP_\xi}, \tag{14}$$

$$\ddot{\eta} + 2\dot{\xi} - U^o_{yy}\eta = a_\eta + a_{SEP_\eta}, \tag{15}$$

$$\ddot{\zeta} - U^o_{zz}\zeta = a_\zeta + a_{SEP_\zeta}, \tag{16}$$

where U^o_{xx}, U^o_{yy}, and U^o_{zz} are the partial derivatives of the gravitational potential evaluated at the collinear libration points, and the solar sail acceleration is defined in terms of three auxiliary variables a_ξ, a_η, and a_ζ.

The solar sail acceleration components are given by

$$a_\xi = a_0 \cos(\omega_\star t)\cos^3(\gamma), \tag{17}$$

$$a_\eta = -a_0 \sin(\omega_\star t)\cos^3(\gamma), \tag{18}$$

$$a_\zeta = a_0 \cos^2(\gamma)\sin(\gamma), \tag{19}$$

where a_0 is the characteristic acceleration. The SEP acceleration components $\boldsymbol{a}_{SEP}$ are used for feedback control as described later.

FEEDBACK LINEARIZING APPROACH TO THE TRACKING IN NONLINEAR SYSTEMS

Objectives

Linearization by feedback is a well-known approach to control nonlinear systems. This method transforms a nonlinear state space model into a new coordinate system where the nonlinearities can

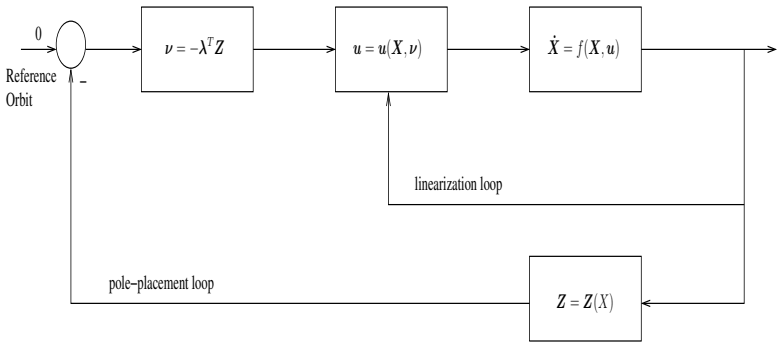

Figure 2. Block Diagram of Feedback Linearization.

be cancelled by feedback. It is a way of transforming system models into equivalent models of simpler form. For example, a change of variables $\boldsymbol{Z} = \Phi(\boldsymbol{X})$ is used to transform the state equation from the $\boldsymbol{X}$-coordinates to the $\boldsymbol{Z}$-coordinates, where the map $\Phi(.)$ must be invertible, such that $\boldsymbol{X} = \Phi^{-1}(\boldsymbol{Z})$ for $\boldsymbol{Z} \in \Phi(D)$ where D is the domain of Φ. Furthermore, the derivatives of $\boldsymbol{X}$ and $\boldsymbol{Z}$ should be continous and therefore the map Φ and its inverse $\Phi^{-1}(.)$ are continously differentiable. Such a map is a diffeomorphism and can be viewed as a generalization of the coordinate transformation. In order to understand this approach, a formal definition is necessary.

Definition 1 *A nonlinear system*

$$\ddot{\boldsymbol{X}} = f(\boldsymbol{X}, \dot{\boldsymbol{X}}) + \boldsymbol{u} \tag{20}$$

where $f : D \to \mathbb{R}^n$ is sufficiently smooth on a domain $D \subset \mathbb{R}^n$ is said to be feedback linearizable (or input-state linearizable) if there exits a diffeomorphism $\Phi : D \to \mathbb{R}^n$, and a nonlinear feedback control law $\boldsymbol{u} = (\boldsymbol{X}, \boldsymbol{\nu})$ such that the new state variables

$$\boldsymbol{Z} = \Phi(\boldsymbol{X}) \tag{21}$$

and the new control input $\boldsymbol{\nu}$ satisfy a linear time-invariant relation

$$\dot{\boldsymbol{Z}} = A\boldsymbol{Z} + B\boldsymbol{\nu} \tag{22}$$

where the pair (A, B) is completely controllable.

Given the nonlinear system of equation (20), the problem of feedback linearization consists of finding, if possible, a change of coordinates of the form of equation (21) and a static state feedback control $\boldsymbol{u} = (\boldsymbol{X}, \boldsymbol{\nu})$, such that (A, B) is controllable. This technique is completely different from a jacobian linearization, on which linear control is based. The block diagram of the feedback linearization is depicted in Figure 2. From equation (1) the motion of the hybrid solar sail in the CRTBP is described by the scalar equations in the form

$$\ddot{\xi} = 2\dot{\eta} + (x_{L_2} + \xi) - (1-\mu)\frac{(x_{L_2} + \xi) + \mu}{r_1^3} - \mu\frac{(x_{L_2} + \xi) - 1 + \mu}{r_2^3} + a_\xi + u_\xi, \tag{23}$$

$$\ddot{\eta} = -2\dot{\xi} + \eta - \left(\frac{1-\mu}{r_1^3} + \frac{\mu}{r_2^3}\right)\eta + a_\eta + u_\eta, \tag{24}$$

$$\ddot{\zeta} = -\left(\frac{1-\mu}{r_1^3} + \frac{\mu}{r_2^3}\right)\zeta + a_\zeta + u_\zeta, \tag{25}$$

where the vector

$$\boldsymbol{u}(t) = \begin{bmatrix} u_\xi & u_\eta & u_\zeta \end{bmatrix}^T \tag{26}$$

is the applied control acceleration due to the SEP thruster.

To develop a feedback linearization scheme, the motion of the hybrid solar sail moving in the CRTBP is separated into linear and nonlinear components, such that

$$\ddot{\xi} = f^{\xi}_{Non-Linear} + f^{\xi}_{Linear} + a_\xi + u_\xi, \tag{27}$$
$$\ddot{\eta} = f^{\eta}_{Non-Linear} + f^{\eta}_{Linear} + a_\eta + u_\eta, \tag{28}$$
$$\ddot{\zeta} = f^{\zeta}_{Non-Linear} + f^{\zeta}_{Linear} + a_\zeta + u_\zeta, \tag{29}$$

where the f functions are defined as the linear and the nonlinear terms in the equations (23), (24) and (25)

$$f^{\xi}_{Non-Linear} = -(1-\mu)\frac{(x_{L_2}+\xi)+\mu}{r_1^3} - \mu\frac{(x_{L_2}+\xi)-1+\mu}{r_2^3}, \tag{30}$$
$$f^{\xi}_{Linear} = 2\dot{\eta} + (x_{L_2}+\xi), \tag{31}$$
$$f^{\eta}_{Non-Linear} = -\left(\frac{1-\mu}{r_1^3} + \frac{\mu}{r_2^3}\right)\eta, \tag{32}$$
$$f^{\eta}_{Linear} = -2\dot{\eta} + (x_{L_2}+\xi), \tag{33}$$
$$f^{\zeta}_{Non-Linear} = -\left(\frac{1-\mu}{r_1^3} + \frac{\mu}{r_2^3}\right)\zeta, \tag{34}$$
$$f^{\zeta}_{Linear} = 0, \tag{35}$$

with $r_1 = \sqrt{((x_{L_2}+\xi)+\mu)^2+\eta^2+\zeta^2}$ $\quad and \quad$ $r_2 = \sqrt{((x_{L_2}+\xi)-1+\mu)^2+\eta^2+\zeta^2}$.

The solar sail acceleration components are given in equations (17), (18) and (19). We then select the SEP control $\boldsymbol{u}(t)$ such that

$$\boldsymbol{u}(t) = \begin{bmatrix} u_\xi \\ u_\eta \\ u_\zeta \end{bmatrix} = -\begin{bmatrix} (x_{L_2}+\xi) - (1-\mu)\frac{(x_{L_2}+\xi)+\mu}{r_1^3} - \mu\frac{(x_{L_2}+\xi)-1+\mu}{r_2^3} - U^o_{xx}\xi \\ -\left(\frac{1-\mu}{r_1^3} + \frac{\mu}{r_2^3}\right)\eta - U^o_{yy}\eta \\ -\left(\frac{1-\mu}{r_1^3} + \frac{\mu}{r_2^3}\right)\zeta - U^o_{zz}\zeta \end{bmatrix} \tag{36}$$

$$+\tilde{\boldsymbol{u}}(t). \tag{37}$$

The equations (23), (24) and (25) then become

$$\ddot{\xi} = 2\dot{\eta} + U^o_{xx}\xi + a_0\cos(\omega_\star t)\cos^3(\gamma) + \tilde{u}_\xi, \tag{38}$$
$$\ddot{\eta} = -2\dot{\xi} + U^o_{yy}\eta - a_0\sin(\omega_\star t)\cos^3(\gamma) + \tilde{u}_\eta, \tag{39}$$
$$\ddot{\zeta} = U^o_{zz}\zeta + a_0\cos^2(\gamma)\sin(\gamma) + \tilde{u}_\zeta. \tag{40}$$

By removing the nonlinear dynamics from the system, the control acceleration vector $\tilde{\boldsymbol{u}}(t)$ is determined such that the desired response characteristics of the linear time-invariant dynamics are produced. In particular, it can be ensured that the displacement distance of the periodic orbit is constant, which provides key advantages for lunar polar telecommunications.

Linearization about a Reference Solution

In this study, the reference trajectory is obtained from the linear analytical solution. Let $\boldsymbol{X}_{ref}(t)$ represent some reference motion that satisfies the system equations (14), (15) and (16), then $\boldsymbol{u}_{ref}(t)$ denotes the control effort required to maintain $\boldsymbol{X}_{ref}(t)$.

The linearization about this reference solution yields a subsystem of the form

$$\dot{\mathbf{X}}(t)_{Linear} = \tilde{A}\mathbf{X}(t)_{Linear} + B\tilde{\boldsymbol{u}}(t), \tag{41}$$

where the matrix B is defined by

$$B = \begin{pmatrix} 0_3 & I_3 \end{pmatrix}^T, \tag{42}$$

and $\tilde{A}$ is determined from the linear dynamics of the solar sail motion such that

$$\tilde{A} = \begin{pmatrix} 0_3 & I_3 \\ K & \Omega \end{pmatrix}, \tag{43}$$

with Ω defined in equation (13). Hence, using feedback to convert a nonlinear state equation into a controllable linear state equation by cancelling the nonlinearities requires the nonlinear state equation to have the form of equation (41).

STABILIZATION AND TRACKING OF FEEDBACK LINEARIZABLE SYSTEMS

After transforming nonlinear dynamics into a linear form, one can easily design controllers for either stabilization or tracking purposes.

Stabilization

Let us consider nonlinear system described by

$$\ddot{\boldsymbol{X}} = f(\boldsymbol{X}, \dot{\boldsymbol{X}}) + \boldsymbol{u}, \tag{44}$$

where $\boldsymbol{X} \in \mathbb{R}^3$ is the state. Let $\boldsymbol{e}(t) = \boldsymbol{X}(t) - \boldsymbol{X}_{ref}(t)$ denote the state error relative to some reference solution, where the reference trajectory

$$\boldsymbol{X}_{ref}(t) = \begin{bmatrix} X_{ref} & Y_{ref} & Z_{ref} \end{bmatrix}^T \tag{45}$$

is given by the analytical solution

$$X_{ref}(t) = x_{Li} + \xi(t), \tag{46}$$
$$Y_{ref}(t) = \eta(t), \tag{47}$$
$$Z_{ref}(t) = \zeta(t), \tag{48}$$

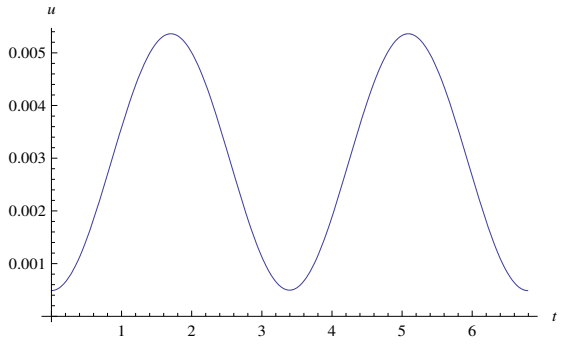

Figure 3. Magnitude of the total control effort.

$(i = 1, 2, 3)$ with

$$\xi(t) = \xi_0 \cos(\omega_\star t), \tag{49}$$
$$\eta(t) = \eta_0 \sin(\omega_\star t), \tag{50}$$
$$\zeta(t) = \zeta_0, \tag{51}$$

which is a solution of the linear equations (14 - 16) with $\boldsymbol{a}_{SEP} = 0$ (pure sail at linear order). $\boldsymbol{a}_{SEP}$ need to cancel the higher order terms in the expansion.

Then differentiate $\boldsymbol{e}(t)$ until the control appears so that

$$\boldsymbol{e}(t) = \boldsymbol{X}(t) - \boldsymbol{X}_{ref}(t), \tag{52}$$
$$\dot{\boldsymbol{e}}(t) = \dot{\boldsymbol{X}}(t) - \dot{\boldsymbol{X}}_{ref}(t), \tag{53}$$
$$\ddot{\boldsymbol{e}}(t) = \ddot{\boldsymbol{X}}(t) - \ddot{\boldsymbol{X}}_{ref}(t), \tag{54}$$
$$= f(\boldsymbol{X}, \dot{\boldsymbol{X}}) + \boldsymbol{u} - \ddot{\boldsymbol{X}}_{ref}(t), \tag{55}$$
$$= -\lambda_1 \dot{\boldsymbol{e}} - \lambda_2 \boldsymbol{e}, \tag{56}$$

and so, we have

$$\boldsymbol{u}(t) = -f(\boldsymbol{X}, \dot{\boldsymbol{X}}) + \ddot{\boldsymbol{X}}_{ref}(t) - \lambda_1 \dot{\boldsymbol{e}} - \lambda_2 \boldsymbol{e}, \tag{57}$$

where $-\lambda_1 \dot{\boldsymbol{e}} - \lambda_2 \boldsymbol{e}$ is the stabilizing term.

Trajectory Tracking

Consider the system given by (44), where our objective is to make the output $\boldsymbol{X} \in \mathbb{R}^3$ track a desired trajectory given by the reference trajectory $\boldsymbol{X}_{ref} \in \mathbb{R}^3$ while keeping the whole state bounded. Therefore, we want to find a control law for the input $\boldsymbol{u} \in \mathbb{R}$ such that, starting from any initial state in a domain $D \subset \mathbb{R}^3$, the tracking error $\boldsymbol{e}(t) = \boldsymbol{X}(t) - \boldsymbol{X}_{ref}(t)$ goes to zero, while the whole state $\boldsymbol{X} \in \mathbb{R}^3$ remains bounded.

Hence, asymtotic tracking will be achieved if we design a state feedback control law to ensure that $\boldsymbol{e}(t)$ is bounded and converges to zero as t tends to infinity.

Thus, the control law

$$\boldsymbol{u}(t) = -f(\boldsymbol{X}, \dot{\boldsymbol{X}}) + \ddot{\boldsymbol{X}}_{ref}(t) - \lambda_1 \dot{\boldsymbol{e}} - \lambda_2 \boldsymbol{e} \tag{58}$$

yields the tracking error equation

$$\ddot{\boldsymbol{e}} + \lambda_1 \dot{\boldsymbol{e}} + \lambda_2 \boldsymbol{e} = 0, \tag{59}$$

where λ_1 and λ_2 are chosen positive constants.

EVALUATION OF HYBRID SAIL PERFORMANCE

In this section we investigate the performance of a hybrid sail system, constituted by a solar sail combined with solar electric propulsion. The simulation was performed around the L_2 point for a period of one month. The magnitude of the total control effort appears in Figure 3. Thus, the control acceleration effort $\boldsymbol{u}$ required to track the reference orbit while rejecting the nonlinearities varies up to 0.005 ($0.1\ mm/s^2$) about the L_2 point. This control acceleration is a continous smooth signal that is much more efficient, in the sense of control effort, compared to the solar sail acceleration. The acceleration derived from the solar sail (denoted by a_ξ, a_η, a_ζ) is plotted in terms of components for one-month orbits in Figure 4 (a), and the SEP acceleration components appears in Figure 4 (b). The control acceleration effort derived from the thruster (denoted by u_ξ, u_η, u_ζ) is order of 10^{-3} - 10^{-4}, while the acceleration derived from the solar sail is approximately 10^{-2}. The small control acceleration from the SEP thruster is then applied to ensure that the displacement of the periodic orbit is constant. The solar sail provides a constant out-of-plane force.

Figure 5 (a) (resp. Figure 5 (b)) illustrates the position error components, denoted by e_ξ, e_η, e_ζ (resp. velocity error components, denoted by $e_{\xi d}, e_{\eta d}, e_{\zeta d}$) under the nonlinear control and the SEP thruster around L_2. These Figures show that the motion is bounded and periodic. This observation implies that the augmented thrust acceleration ensures a constant displacement orbit. The reference orbit above L_2 and the orbit resulting from tracking the reference orbit using the nonlinear control and the SEP thruster around L_2 are also depicted in Figure 6 (a) and 6 (b) respectively.

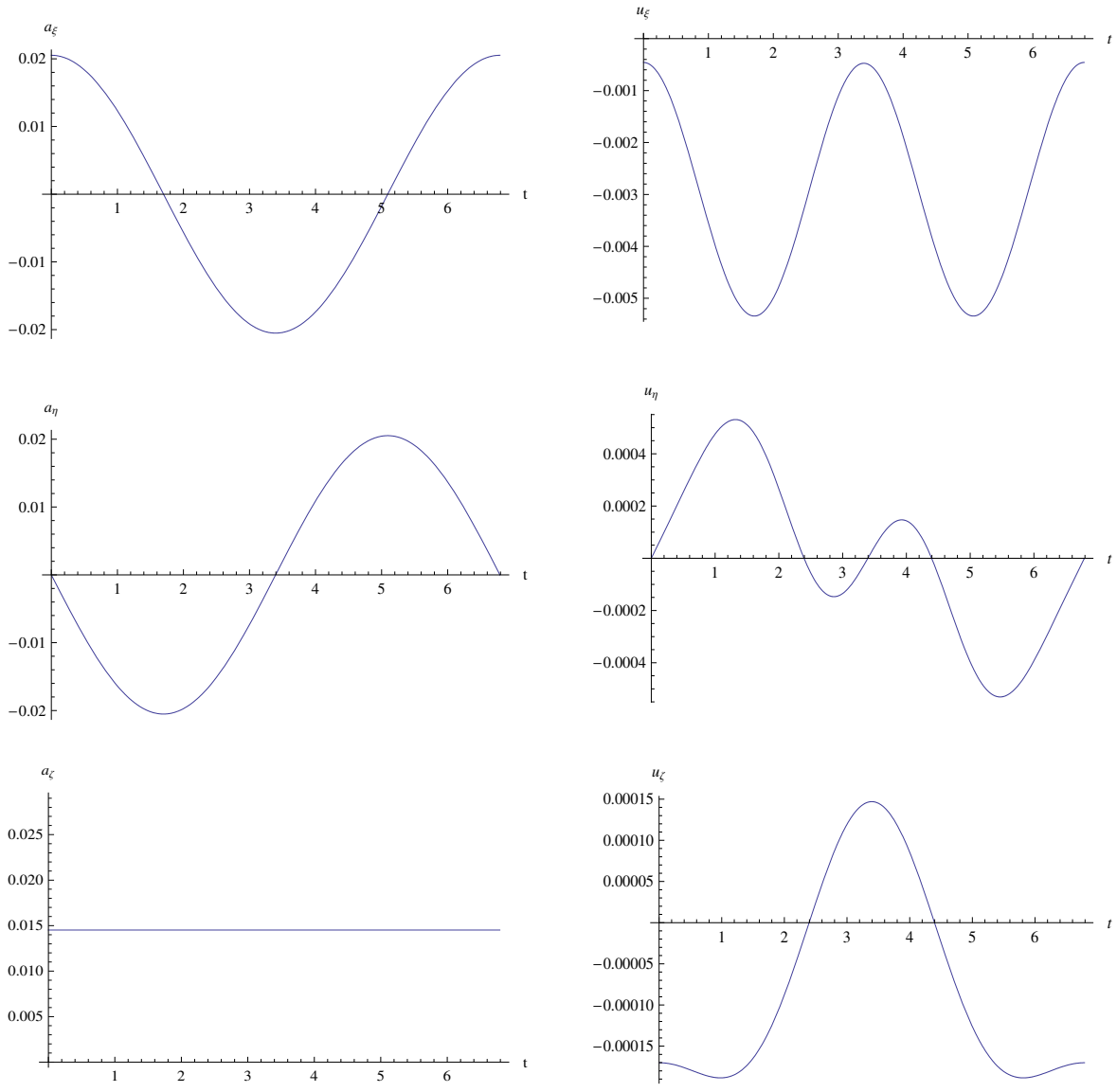

Figure 4. (a) **Acceleration derived from the solar sail;** (b) **Acceleration derived from the thruster.**

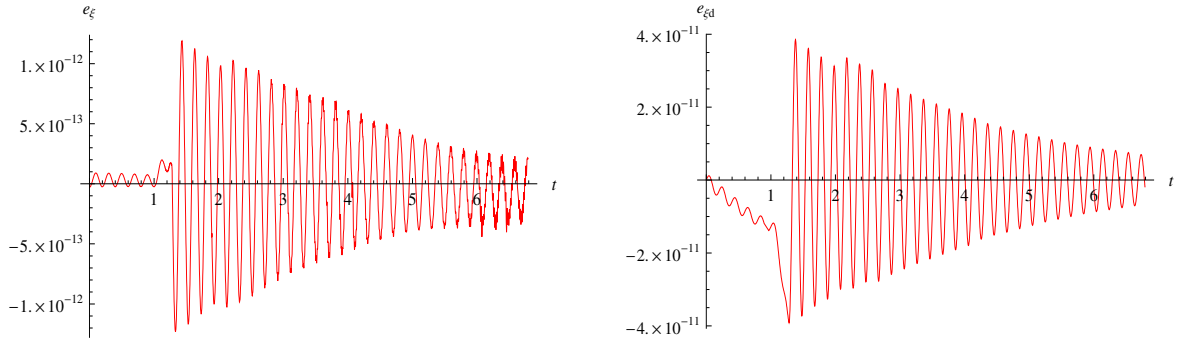

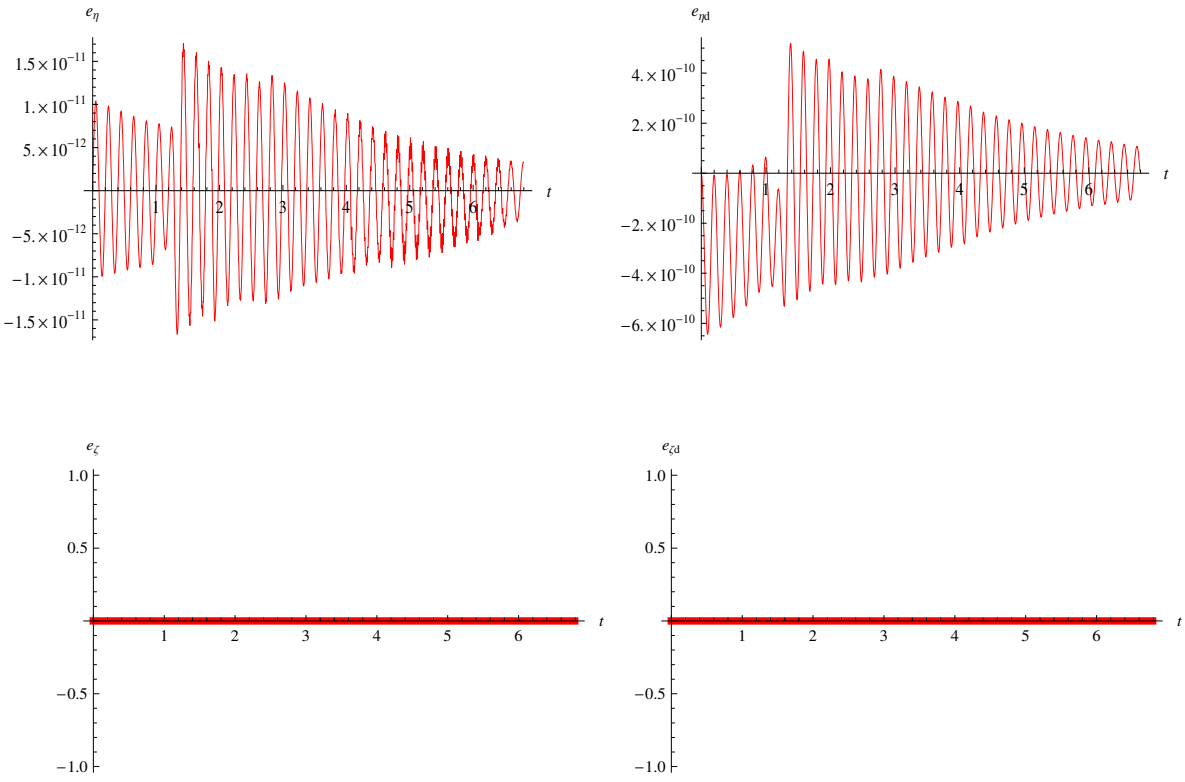

(a) (b)

Figure 5. (a) **Position Errors;** (b) **Velocity Errors.**

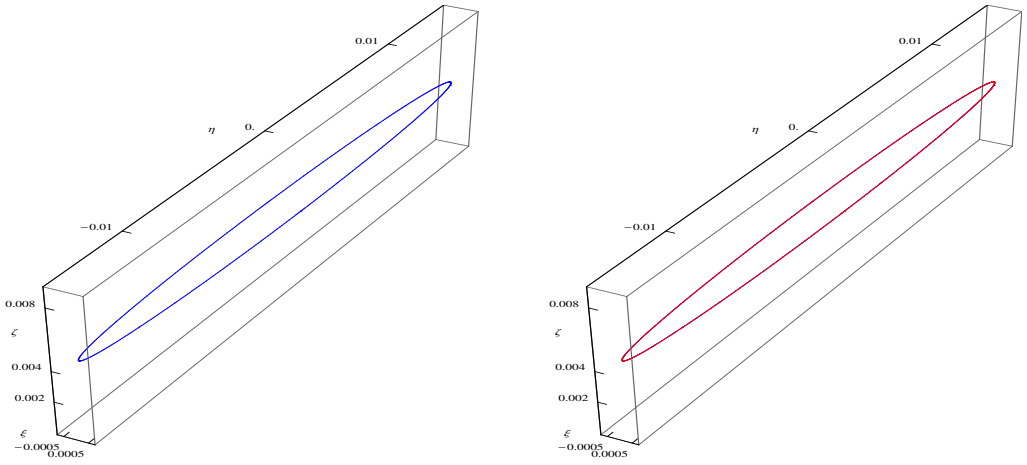

(a) (b)

Figure 6 (a) **Reference orbit above** L_2**;** (b) **Orbit resulting from tracking the reference orbit using the nonlinear control and SEP thruster around** L_2**.**

Propellant Usage

Propellant usage for the SEP thruster is proportional to the total ΔV, which is the integration over time of the magnitude of the control acceleration acceleration produced by using the SEP thruster so that

$$\Delta V = \int_0^{2\pi/\omega_\star} |\boldsymbol{u}| dt. \tag{60}$$

The total ΔV_{Total} over a 5 years mission is given by

$$\Delta V_{Total} = \Delta V per\ orbit \times no, \tag{61}$$

where no is the total number of orbits. Once the total ΔV is computed, the propellant usage can be found using the rocket equation.

Let us define the mass m of the rocket at a time t, as a function of the initial mass m_i, ΔV and the effective exhaust velocity $v_e = I_{sp} \cdot g$,

$$m = m_i e^{-\Delta V/g \cdot I_{sp}}. \tag{62}$$

The mass of propellant is then the difference between the initial and the final masses

$$m_{prop} = m_i - m = m_i(1 - e^{-\Delta V_{Total}/g \cdot I_{sp}}), \tag{63}$$

where I_{sp} is the specific impulse ($\approx 3000\ sec$ for an electric thruster).

Assume a specific impulse of $I_{sp} = 3000\ sec$ and an initial mass of $m_i = 500\ kg$, we have the average ΔV per orbit of approximately $23\ m/s$. Then, the total ΔV per orbit over 5 years is 1536 m/s. The consumed propellant mass is then $m_{prop} = 25\ kg$. The parameters are summarized in Table 1.

Table 1. Summary of Parameters.

Parameter	Description	Value
$m_i\ (kg)$	Initial Mass	500
$I_{sp}\ (sec)$	Specific Impulse	3000
$\Delta V_{Total}\ (m/s)$	Total ΔV over 5 years	1536
$m_{prop}(kg)$	Propellant Mass Consummed	25

CONCLUSIONS

A hybrid concept for displaced periodic orbits in the Earth-Moon system has been developed. A feedback linearization was used to perform stabilization and trajectory tracking for nonlinear systems. The idea of this control is to transform a given nonlinear system into a linear system by use of a nonlinear coordinate transformation and nonlinear feedback. The augmented thrust acceleration is than applied to ensure a constant displacement periodic orbit, which provides key advantages for

lunar polar telecommunications. A stabilizing approach is then introduced to increase the damping in the system and to allow a higher gain in the controller. Theoretical and simulation results show good performance, with modest propellant mass requirements.

ACKNOWLEDGMENTS

This work was funded by the European MCRTN AstroNet, Contract Grant No. MRTN-CT-2006-035151.

REFERENCES

[1] C. R. McInnes, *Solar sailing: technology, dynamics and mission applications*. London: Springer Praxis, 1999.

[2] T. Waters and C. McInnes, "Periodic Orbits Above the Ecliptic in the Solar-Sail Restricted Three-Body Problem," *J. of Guidance, Control, and Dynamics*, Vol. 30, No. 3, 2007, pp. 687–693.

[3] J. Simo and C. R. McInnes, "Solar sail trajectories at the Earth-Moon Lagrange points," *In 59th International Astronautical Congress*, Glasgow, Scotland, 29 Sep - 03 Oct 2008.

[4] C. McInnes, "Solar sail Trajectories at the Lunar L_2 Lagrange Point," *J. of Spacecraft and Rocket*, Vol. 30, No. 6, 1993, pp. 782–784.

[5] M. Ozimek, D. Grebow, and K. Howell, "Solar Sails and Lunar South Pole Coverage," *In AIAA/AAS Astrodynamics Specialist Conference and Exhibit*, Honolulu, Hawaii,August 2008.

[6] H. Baoyin and C. McInnes, "Solar sail halo orbits at the Sun-Earth artificial L_1 point," *Celestial Mechanics and Dynamical Astronomy*, Vol. 94, No. 2, 2006, pp. 155–171.

[7] H. Baoyin and C. McInnes, "Solar sail equilibria in the elliptical restricted three-body problem," *Journal of Guidance, Control and Dynamics*, Vol. 29, No. 3, 2006, pp. 538–543.

[8] H. Baoyin and C. McInnes, "Solar sail orbits at artificial Sun-Earth Lagrange points," *Journal of Guidance, Control and Dynamics*, Vol. 28, No. 6, 2005, pp. 1328–1331.

[9] C. R. McInnes, "Artificial Lagrange points for a non-perfect solar sail," *Journal of Guidance, Control and Dynamics*, Vol. 22, No. 1, 1999, pp. 185–187.

[10] C. McInnes, A. McDonald, J. Simmons, and E. McDonald, "Solar sail parking in restricted three-body systems," *Journal of Guidance, Control and Dynamics*, Vol. 17, No. 2, 1994, pp. 399–406.

[11] M. Leipold and M. Götz, "Hybrid Photonic/Electric Propulsion," *Kayser-Threde, TR SOL4- TR-KTH-0001*, Munich, Jan. 2002, ESA Contract No. 15334/01/NL/PA.

[12] G. Mengali and A. A. Quarta, "Trajectory Design with Hybrid Low-Thrust Propulsion system," *Journal of Guidance, Control, and Dynamics*, Vol. 30, No. 2, March-April 2007, pp. 419–426.

[13] S. Baig and C. McInnes, "Artificial Three-Body Equilibria for Hybrid Low-Thrust Propulsion," *J. of Guidance, Control, and Dynamics*, Vol. 31, No. 6, November-December 2008, pp. 1644–1655.

[14] V. Szebehely, *Theory of Orbits: the restricted problem of three bodies*. New York and London: Academic Press, 1967.

[15] R. Farquhar, "The Control and Use of Libration-Point Satellites," *Ph.D. Dissertation, Stanford University*, 1968.

[16] A. E. Roy, *Orbital Motion*. Bristol and Philadelphia: Institute of Physics Publishing, 2005.

[17] F. Vonbun, ""A Humminbird for the L_2 Lunar Libration Point"," *Nasa TN-D-4468*, April 1968.

[18] R. Thurman and P. Worfolk, "The geometry of halo orbits in the circular restricted three-body problem," *Technical report GCG95, Geometry Center, University of Minnesota*, 1996.

[19] G. Gómez, J. Llibre, R. Martínez, and C. Simó, *Dynamics and Mission Design Near Libration Points*, Vol. I, II. Singapore.New Jersey.London.Hong Kong: World Scientific Publishing Co.Pte.Ltd, 2001.

[20] G. Gómez, A. Jorba., J.Masdemont, and C. Simó, *Dynamics and Mission Design Near Libration Points*, Vol. III, IV. Singapore.New Jersey.London.Hong Kong: World Scientific Publishing Co.Pte.Ltd, 2001.

[21] J. Breakwell and J. Brown, "The 'halo' family of 3-dimensional periodic orbits in the Earth-Moon restricted 3-body problem," *Celestial Mechanics*, Vol. 20, 1979, pp. 389–404.

[22] D. L. Richardson, "Halo orbit formulation for the ISEE-3 mission," *J. Guidance and Control*, Vol. 3, No. 6, 1980, pp. 543–548.

[23] K. Howell, "Three-dimensional, periodic, 'halo' orbits," *Celestial Mechanics*, Vol. 32, 1984, pp. 53–71.

[24] K. Howell and B. Marchand, “”Natural and Non-Natural Spacecraft Formations Near L_1 and L_2 Libration Points in the Sun-Earth/Moon Ephemerics System”,” *Dynamical Systems: An International Journal*, Vol. 20, No. 1, March 2005, pp. 149–173.

[25] R. Farquhar, “The utilization of Halo orbits in advanced lunar operations,” *Nasa technical report*, 1971.

[26] R. Farquhar and A. Kamel, “Quasi-periodic orbits about the translunar libration point,” *Celestial Mechanics*, Vol. 7, 1973, pp. 458–473.

[27] J.-J. E. Slotine and W. Li, *Applied Nonlinear Control*. Englewood Cliffs, New Jersey 07632: Prentice Hall, 1991.